

Relaxations in Thermosets. 23. Dielectric Studies of Curing Kinetics of an Epoxide with Diamines of Varying Chain Lengths

M. G. Parthun and G. P. Johari*

Department of Materials Science and Engineering, McMaster University,
Hamilton, Ontario L8S 4L7, Canada

Received October 17, 1991; Revised Manuscript Received February 3, 1992

ABSTRACT: The curing kinetics of two thermosets of diglycidyl ether of Bisphenol A with propylenediamine and hexamethylenediamine have been studied at several temperatures and measurement frequencies. The results have been analyzed both in the permittivity and complex modulus formalisms, and a general pattern of curing kinetics has been observed. At the earlier stages of curing, the dc conductivity decreases according to a scaling law with a critical exponent which increases with the curing temperature. This decrease can also be described by a singularity equation. The analysis has been used to obtain the gelation time of the thermoset and its variation with the temperature and molecular size of the curing agent. The complex permittivity irreversibly changes as the thermoset cures, but these changes are observable only in the postgel period. The permittivity follows a stretched exponential relaxation function with a curing parameter whose value is both temperature and chain length dependent. The relaxation time increases with curing time according to a curve with a sigmoidal shape. This curve shifts to shorter times with an increase in the curing temperature. Measurements for different frequencies show that the various parameters for the curing kinetics are independent of the frequency of measurements. These results are discussed, and information on the effects of molecular chain length on the curing kinetics has been obtained.

I. Introduction

Our earlier studies on thermosets have shown that both its sol \rightarrow gel conversion and vitrification can be characterized by dielectric measurements.¹⁻⁵ The studies also revealed that the dielectric consequences of chemical changes during the curing of a thermoset are analogous to the frequency dependence of complex permittivity of an amorphous solid at a fixed temperature near T_g and that the curing parameter, which was used to represent the curing time-dependence of the complex permittivity, varied with both the curing temperature and the nature of the cross-linking agent. The latter was interpreted to seek a connection between the curing parameters and the distribution of reaction rates.⁵

The chemical reactions that convert a liquid into a rigid network polymer depend upon the diffusion coefficients of the reacting species as a whole and the steric hindrance and the electronic charge distribution of the reacting groups, and, even for molecules of virtually similar size, the time for isothermal curing needed to achieve a dielectrically equivalent state differs by a considerable amount. As part of our continuing studies of thermoset polymers, we have measured the effect of the curing agent's molecular size on the kinetics of gelation and vitrification. For this purpose two linear chain diamines, namely, propylenediamine and hexamethylenediamine, with three and six CH_2 groups between the two amine groups, respectively, were chosen. This paper describes the dielectric behavior of epoxide-based thermosets during their curing with the two amines and the effect of temperature on the curing kinetics.

II. Experimental Methods

Samples of thermosets were prepared by mixing at room temperature 1 mol of propylenediamine (PDA) or hexamethylenediamine (HMDA) with 2 mol of diglycidyl ether of Bisphenol A (DGEBA) in a 5-mm-diameter glass vial. PDA and HMDA of >99% purity were purchased from Aldrich Chemical Co., and a commercial sample of DGEBA, under the name of EPON 828, was donated to us by Shell Petroleum. EPON 828 has been

carefully characterized by LeMay, Swetlin, and Kelley,⁶ and its properties have been listed by Choy and Plazek.⁷ Its $M_n = 380$, $n = 0.14$, $T_g = 259$ K, functionality = 2.0, and soluble fraction of resin completely cured with diaminodiphenyl sulfone is 0.3 w/w %.

The PDA mixture was mechanically mixed at room temperature and the HMDA mixture at 313 K when both were very fluid. A parallel capacitor containing 18 rigid plates was carefully immersed in the solution, and the absence of any air bubble in the sample and between the plates was ensured. The glass vial was electrically shielded and transferred to a cavity drilled in a massive aluminum block whose temperature could be maintained within ± 0.1 K. A copper-constantan thermocouple was immersed in the solution with its junction held in contact with the ceramic spacer of the capacitor.

The dielectric measurement assembly, the related equipment, and the procedure were the same as described in earlier papers.¹⁻⁵ Briefly, a general radio Gen Rad 1689 Digibridge which was interfaced with a personal computer was used for automatic data collection at intervals of 1 min. The accuracy of measurement was 0.1% for capacitance and 1% for conductance. All data were collected after 100 s of the attainment of thermal equilibrium.

III. Results

(i) Dielectric Measurements during Isothermal Curing. The changes in the dielectric properties of the DGEBA-PDA and DGEBA-HMDA thermosets measured at 1-kHz frequency during its isothermal curing at 294.9, 303.8, 315.5, 323.7, 335.0, and 346.0 K and 284.3, 296.5, 304.2, 312.3, 324.3, and 336.5 K are shown as plots of permittivity, ϵ' , and loss, ϵ'' , against the logarithm of curing time, t , in Figures 1 and 2, respectively. The shapes of the curves in these figures are typical for a thermoset's curing, as earlier studies have shown,¹⁻⁵ and are qualitatively similar for each temperature of cure.

At short times of cure, ϵ' decreases slightly, approaching a plateau value as the curing time increases. The plateau is interrupted by a sharp step decrease, following which there is an approach to a limiting value at long times, here defined as $\epsilon'(t \rightarrow \infty)$. As seen in Figures 1 and 2, when the curing temperature is increased, the position of the step

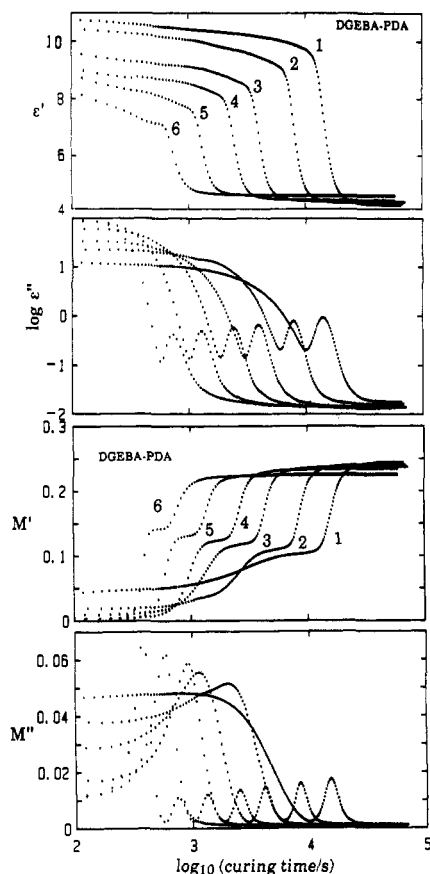


Figure 1. Dielectric permittivity and loss, and the real and imaginary components of the electrical modulus M' and M'' , measured at a frequency of 1 kHz of a DGEBA-PDA thermoset plotted against time during their isothermal curing at several temperatures. The numbers next to the curves correspond to the curing temperatures as listed in Table I.

decrease shifts toward shorter times, and the corresponding magnitude of the step is decreased.

In Figures 1 and 2, ϵ'' begins at a plateau value during the initial stages of cure. The plateau gives way to a decrease toward a local minimum as curing progresses, which is followed by a peak. Ultimately, ϵ'' decreases toward a limiting value at long times, defined as $\epsilon''(t \rightarrow \infty)$. The initial plateau in ϵ'' increases in height, and, as the curing temperature is raised, the corresponding minimum and peak are shifted to shorter times, with the magnitudes of the minimum increasing and those of the peak decreasing.

In order to determine the effect of curing temperature on the dielectric permittivity, it is necessary to determine $\epsilon'(t \rightarrow \infty)$, which is taken as the value of permittivity from the asymptote drawn to the plateau which occurs prior to the step decrease. This value and the value of permittivity at long times, $\epsilon'(t \rightarrow \infty)$, are listed in Table I for the DGEBA-PDA and DGEBA-HMDA thermosets. Additionally, the value of ϵ'' at its peak denoted by ϵ''_{\max} and the time taken to reach the peak, $t_{\text{peak}}(\epsilon'')$, are also included in Table I.

(ii) Complex Electrical Modulus during Isothermal Curing. A thermosetting liquid has a finite electrical conductivity. This is attributed to the diffusion of free ions which either are present as impurities in the resin and the curing agent and/or have been formed on dissociation of the weakly-ionic curing agent. The impurities in the resin and the curing agent are usually the remains of catalysts and degradation products, and most of these are either alkali cations or halide anions. In some cases water may also be present as an impurity, and this, on dissociation, can provide H^+ and OH^- ions. A second

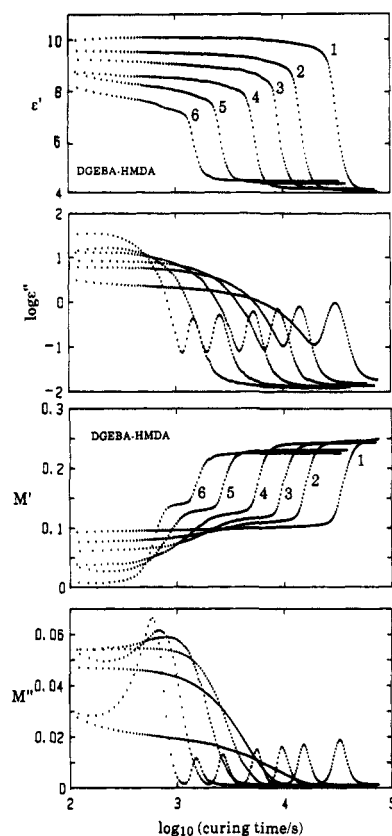


Figure 2. Dielectric permittivity and loss, and the real and imaginary components of the electrical modulus M' and M'' , measured at a frequency of 1 kHz of a DGEBA-HMDA thermoset plotted against time during the isothermal curing at several temperatures. The numbers next to the curves correspond to the curing temperatures as listed in Table I.

mechanism is protonic conduction along the H bonds formed between the amine or hydroxyl curing agent molecules when they form an H-bonded network. As the liquid cures, the increase in the viscosity as a result of cross-linking between the resin and the curing agent slows the ionic transport, while the chemical reactions involved in the cross-linking effectively prevent the formation of H bonds required for the protonic conduction. Thus the conductivity decreases as a result of two effects, namely, (i) an increase in the viscosity according to the Stokes-Einstein equation and (ii) the removal of a mechanism for protonic conduction.

In order to examine the conductivity behavior during the curing of a thermoset, it is useful to analyze the data in such a way that the extraneous effects of the electrode polarization, albeit small, can be eliminated. A representation in terms of the complex electrical modulus, defined as $M^* = 1/\epsilon^*$, allows the transformation of the dielectric data from the complex permittivity, ϵ^* , spectra to the complex modulus, M^* , spectra. This largely eliminates the influence of electrode polarization, as shown by Macedo et al.⁸ and Moynihan et al.,⁹ and thus allows measurements of the dc conductivity.

In the theoretical developments pertaining to the curing kinetics of thermosets, Mangion and Johari⁴ have shown that an analysis in terms of M^* is particularly useful for determining the dc conductivity of a thermoset at any time during its cure since the frequency spectra at a given (fixed) instant of cure, which are necessary for determining the dc conductivity, have been difficult to measure. Time domain reflectometry in which a Fourier transform of the step response to the electrical voltage is used to determine the permittivity spectra from 10^7 to 10^{10} Hz by

Table I
Features of the Dielectric Behavior of DGEBA-Based Thermosets Measured for a Fixed Frequency of 1 kHz during Their Isothermal Curing at Different Temperatures

T_{cure}/K	$\epsilon'(t \rightarrow 0)$	$\epsilon'(t \rightarrow \infty)$	$t(\epsilon''_{\text{max}})/\text{ks}$	ϵ''_{max}	M_{∞}	$M''_{\text{peak},2}$	curve no. ^a
DGEBA-PDA							
294.9	9.65	4.50	13.95	0.90	0.243	0.017	1
303.8	9.10	4.60	7.80	0.76	0.239	0.016	2
315.5	8.45	4.50	3.96	0.63	0.236	0.014	3
323.7	8.10	4.60	2.40	0.57	0.233	0.013	4
335.0	7.70	4.65	1.27	0.48	0.224	0.012	5
346.0	7.19	4.60	0.73	0.40	0.223	0.011	6
DGEBA-HMDA							
284.3	9.50	4.50	30.6	0.94	0.246	0.019	1
296.5	8.85	4.50	14.2	0.78	0.245	0.017	2
304.2	8.35	4.50	9.05	0.68	0.242	0.016	3
312.3	7.93	4.45	5.28	0.59	0.241	0.015	4
324.3	7.60	4.60	2.60	0.50	0.230	0.013	5
336.5	7.10	4.65	1.46	0.42	0.225	0.011	6

^a These numbers refer to the temperature of cure for the two thermosets as denoted in Figures 1–6.

a sampling technique has been used for the measurement of the high-frequency behavior of thermosets at any instant of cure, but this technique does not allow for the measurement of dc conductivity, as Tombari and Johari¹⁰ have observed. There are further limitations in that this method presently seems useful only for studies at megahertz frequencies or higher, for which the changes in the dielectric properties occur in a relatively short time, which makes it necessary to restrict measurements to low temperatures.

The measured ϵ' and ϵ'' were therefore converted to M' and M'' by

$$M^* = 1/\epsilon^* \quad \text{where } \epsilon^* = \epsilon' - i\epsilon''; \quad M^* = M' + iM'' \quad (1)$$

which gives

$$M' = \frac{\epsilon'}{(\epsilon')^2 + (\epsilon'')^2} \quad (2)$$

$$M'' = \frac{\epsilon''}{(\epsilon')^2 + (\epsilon'')^2} \quad (3)$$

The calculated M' and M'' for the two thermosets, measured at 1-kHz frequency during their isothermal curing at different temperatures, are plotted against logarithmic time also in Figures 1 and 2. Since the conductivity is equal to $\omega\epsilon_0\epsilon''$, where ϵ_0 is the permittivity of free space ($=8.8514 \text{ pF/m}$), its plots are similar in shape to those of ϵ'' against log (time) seen in Figures 1 and 2 and therefore are not included here.

The plots of M' against log (time) for the isothermal curing of the two thermosets in Figures 1 and 2 are qualitatively similar in shape, showing an increase which occurs in two steps toward a limiting value, $M_{\infty} = 1/\epsilon_{\infty}$. The height of the first step increases as the curing temperature is raised, and the corresponding height of the second step that follows decreases. Concomitantly, both steps appear at shorter times. The width of the first plateau separating the steps in these figures decreases as the curing temperature is increased.

The corresponding plots of M'' against log (time) in Figures 1 and 2 show two peaks. As the temperature of cure is increased, the positions of the two peaks shift to shorter times and the height of the first peak increases and its shape broadens. Concomitantly, the second peak also shifts to shorter times, its peak height decreases, and its shape becomes narrower. These observations are summarized in Table I where $t_{\text{peak},1}(M'')$ refers to the time

to reach the first peak in the M'' plot and $t_{\text{peak},2}(M'')$ refers to the time to reach the second peak.

IV. Discussion

(i) Isothermal Curing Kinetics Measured at a Fixed Frequency. (a) Electrical Modulus and dc Conductivity. We first consider the change in the dc conductivity of the two thermosets during their curing process. The electrical modulus data can be used to determine the values of the dc conductivity of the thermosets during their isothermal cure in the following manner. The measured conductivity of a dielectric material is given by

$$\sigma = \sigma_0 + \sigma_{\text{dip}} \quad (4)$$

where σ_0 is the dc conductivity and σ_{dip} is the ac or dipolar conductivity. σ_{dip} is equal to $\omega\epsilon_0\epsilon''_{\text{dip}}$ where ω is the angular frequency and ϵ_0 the permittivity of a vacuum ($=8.8514 \text{ pF/m}$). In the beginning of the cure the viscosity of the thermoset liquid is less than 10 P, which means that its shear relaxation time is of the order 10^{-9} s , since $\tau = \eta/G$ and G is about 10^{10} Pa . If the relaxation process is represented by the Debye equation, this would correspond to $\epsilon'' = 10^{-5}$, or $\sigma_{\text{dip}} = 55.6 \times 10^{-14} \text{ S m}^{-1}$, for a 1-kHz measurement frequency with a $\Delta\epsilon$ of ~ 10 .

From the plots of ϵ'' against log (time) shown in Figures 1 and 2, the value of ϵ''_{dip} is 10^{-5} , which is 3–4 orders of magnitude less than the measured value and therefore can be assumed as negligible. Thus in the beginning of the curing process $\epsilon^*(t)$ and $M^*(t)$ have contributions only from $\sigma_0(t)$.

For a Maxwellian conductivity process, according to which the relaxation time is equal to the product of the capacitance and resistance, $M^*(t)$ is written as

$$M^*(t) = \frac{M_s(t) i\omega\tau_{\sigma}(t)}{1 + i\omega\tau_{\sigma}(t)} \quad (5)$$

where $M_s(t)$ is the limiting value of M' and $\tau_{\sigma}(t)$ is the Maxwellian conductivity relaxation time given by

$$\tau_{\sigma}(t) = \frac{\epsilon_0\epsilon_s(t)}{\sigma_0(t)} \quad (6)$$

where $\epsilon_s(t)$ is the static permittivity at time t and ϵ_0 is as defined previously.

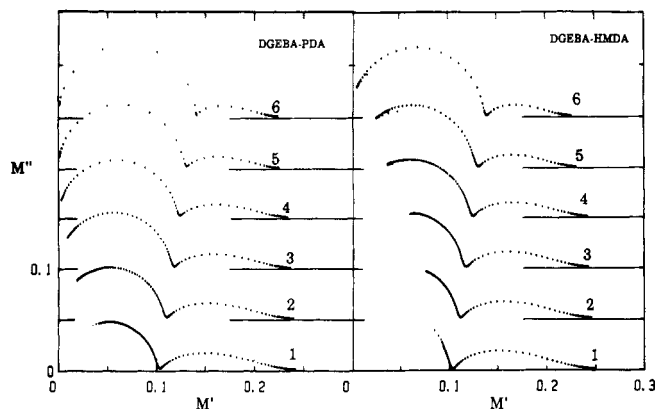


Figure 3. Complex plane plots of M'' against M' for the isothermal cure of the DGEBA-PDA and DGEBA-HMDA thermosets, as measured at a frequency of 1 kHz. The numbers next to the curves correspond to the curing temperatures as listed in Table I.

Since $\epsilon_s(t)$ remains essentially constant with time during the early period of cure and since $\sigma_0 = \omega \epsilon_0 \epsilon''$

$$\tau_c(t) = \frac{1}{\omega \tan \delta(t)} \quad (7)$$

Accordingly, $M^*(t)$ in eq 5 becomes invariant of one's choice of ω or τ_c as variable. Separating eq 5 into its real and imaginary components

$$M'(t) = \frac{M_s(t) \omega^2 \tau_c^2(t)}{1 + \omega^2 \tau_c^2(t)} \quad (8)$$

$$M''(t) = \frac{M_s(t) \omega \tau_c(t)}{1 + \omega^2 \tau_c^2(t)} \quad (9)$$

Combining eqs 8 and 9 yields

$$[M''(t)]^2 + [M'(t) - M_s/2]^2 = [M_s/2]^2 \quad (10)$$

According to eq 10, a complex plane plot of M'' against M' should be a semicircle of radius $M_s/2$, whose center lies on the M' axis at the point $M' = M_s/2$, if the contributions to M' were strictly due to the dc conductivity. Thus, if the observed behavior follows eq 10, the dc conductivity, $\sigma_0(t)$, can be calculated at any time during the cure from the value of $\tan \delta(t)$ (or $\epsilon''(t)/\epsilon'(t)$), ω , and $\epsilon_s(t)$, using eqs 6 and 7.

The complex plane plots of M'' against M' measured for a fixed frequency of 1 kHz during the isothermal curing of the DGEBA-PDA and DGEBA-HMDA thermosets are shown in Figure 3. The curing temperatures here are the same as those for the plots in Figures 1 and 2. These plots for the two thermosets also show similar behavior, i.e., that at the initial stages of a thermoset's curing the curves are described by a semicircle. This means that, in the initial stages of the curing process, the dc conductivity is the dominant term in eq 4. At longer times, deviations from the semicircle occur as contributions from σ_{dip} to M'' become significant. After the semicircle, or at longer times, a second, skewed arc appears which corresponds to the dipolar reorientation process. This will be discussed in section IV(c).

(b) dc Conductivity and Thermoset's Gelation. The shape of the complex plane plots of M'' against M' suggests that it is the decreases in the dc conductivity, rather than the change in the contribution from dipolar reorientation, which dominate the dielectric behavior of a thermoset in the initial stages of its isothermal curing. Therefore, an

analysis of the dc conductivity of the thermoset during its curing process can only be made up to a time before the minimum in ϵ'' (or equivalently in σ) appears in the plots seen in Figures 1 and 2, where its value is small and approaches zero. As mentioned earlier, this finite but small value is due to the diffusion of ionic impurities and protons in the liquid before a completely cross-linked network of covalent bonds is formed.

The decrease in the dc conductivity during the isothermal curing of a thermoset has been described in terms of a critical phenomenon, in which the irreversible sol-gel conversion occurs by a negative feedback process between molecular diffusion and chemical reactions. As a thermoset cures, the decrease in the molecular diffusion rate on cross-linking of molecules causes an increase in the viscosity of the liquid. At a time when sufficient cross-linking has occurred to form an infinitely connected network, the macroscopic viscosity formally approaches an infinite value with a mechanical modulus of about 10^7 Pa, corresponding to that of the gelled state. In theoretical treatment of the transport properties of materials in terms of scaling concepts, Stauffer et al.¹¹ and Djabourov¹² have shown that the molecular transport properties follow a power law of the form

$$p(t) \propto [(t_{gel} - t)/t_{gel}]^x \quad (11)$$

where $p(t)$ is a transport property of the material, t_{gel} is the time required to form a gel or infinitely cross-linked network, and x is a constant, also known as the critical exponent, which describes the rate of approach of the transport properties toward the singularity point at t_{gel} . As mentioned earlier here, the dc conductivity in a liquid thermoset results from impurity ion motions and protonic conduction along H bonds. Therefore, as chemical reactions continue to occur during the curing process, both effects concurrently diminish, the former as a result of the increase in viscosity and the latter owing to the breakup of the H-bonded network of the curing agent. Mangion and Johari⁴ have shown that the dc conductivity of a thermoset during its isothermal curing changes according to eq 11 such that

$$\sigma_0(t) = \sigma_0(t \rightarrow 0) [(t_{gel} - t)/t_{gel}]^x \quad (12)$$

where $\sigma_0(t \rightarrow 0)$ is the dc conductivity of the unreacted thermoset liquid at $t_{cure} \rightarrow 0$, and t_{gel} is the time required to form the gelled network structure.

The conductivity data were fitted to eq 12 using a reiterative procedure until a value chosen for t_{gel} gave minimum mean-square deviations of the data from those calculated. Comparisons between the experimental curves for the conductivity measured during the isothermal curing of the DGEBA-PDA and DGEBA-HMDA thermosets at different temperatures and the best-fit curve calculated from eq 12 are shown in the plots of σ against $\log(t)$ in Figure 4. As is seen, the fit in all cases is satisfactory, with deviations occurring at longer times where, as expected, contributions from σ_{dip} become significant.

In an alternative approach proposed by Johari and Mangion,³ the dc conductivity can also be described by an equation of the form

$$\sigma_0(t) = A \exp[-B/(t_0 - t)] \quad (13)$$

where t_0 is the time when σ_0 would formally approach zero. A and B are temperature-dependent empirical parameters which determine the magnitude and rate at which the conductivity approaches a singularity at t_0 . A ,

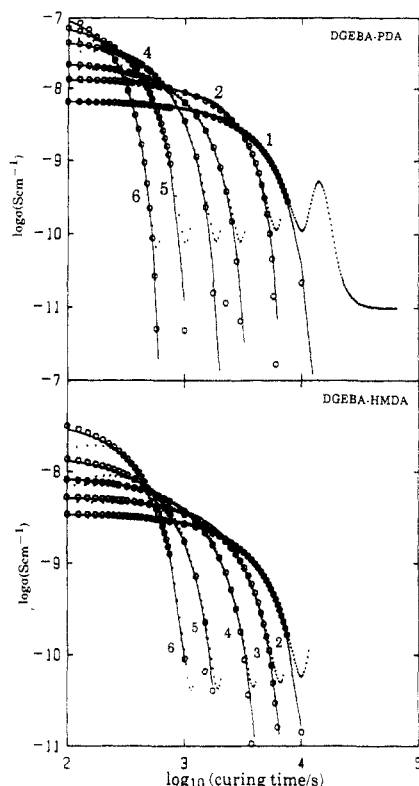


Figure 4. Conductivities of the DGEBA-PDA and DGEBA-HMD thermosets, measured at a frequency of 1 kHz, plotted against time for isothermal cure. The numbers next to the curves correspond to the curing temperatures as listed in Table I. The circles are the data calculated from the power law, given by eq 12, and the full lines are those calculated from the singularity equation, eq 13, using the parameters listed in Table II.

B , and t_0 were also determined by a reiterative procedure, and the σ_0 calculated from eq 13 for each set of data obtained during the isothermal curing of the DGEBA-PDA and DGEBA-HMDA thermosets are plotted in Figure 4. Evidently, the calculated σ_0 is in satisfactory agreement with the experimental data and is comparable with those calculated from the power law in eq 12. A summary of the values of the parameters, t_{gel} , t_0 , $\sigma_0(t \rightarrow 0)$, x , A , and B used for the analyses is given in Table II.

Since the dc conductivity seems equally well-described by the power law in eq 12 and a singularity equation in eq 13, their relative merits for the phenomenology of gelation may be considered by examining the values of the parameters t_{gel} and t_0 . For curing at all temperatures of both thermosets, the value of t_{gel} listed in Table II is less than the time to reach the peak in ϵ'' at 1 kHz, denoted as $t_{peak}(\epsilon'')$ in Table I, while that of t_0 is greater than $t_{peak}(\epsilon'')$. Thus, t_0 may be associated with the vitrification time t_{vit} , which suggests that the singularity at t_0 in eq 13 is due to the approach of the microscopic viscosity toward a formally infinite value instead of the time for gelation when the relaxation time is less than 0.1 μ s. The value of t_{gel} taken as the time to form a gelled structure is always less than t_0 , which seems reasonable because in all our experiments the curing temperature was such that gelation occurred prior to vitrification.

(c) Dipolar Relaxation. In the analysis of the complex electrical modulus, the complex plane plots of M'' against M' for the isothermal curing of thermosets show two distinct arcs: the first, a semicircular arc and the second a skewed arc which becomes progressively more skewed at longer times. The semicircular arc describes the change in the dc conductivity of the thermoset with time prior to gelation. The skewed arc appears at times after the time

for the minimum in ϵ'' , and, as such, it represents the change in the dielectric properties that occurs after the dc conductivity becomes negligible or effectively zero. This dipolar relaxation process is more clearly seen in the complex plane plots of ϵ'' against ϵ' for the two thermosets shown in Figure 5.

A method for analyzing the dielectric relaxation in the postgel period during the isothermal curing of thermosets has been developed by Johari and Mangion³ in terms of the changes in the ϵ^* spectra. They have shown that a general representation of the permittivity spectra ϵ^* , at any instance of cure, t , in the absence of dc conductivity is given as

$$\epsilon^*(t) = \epsilon_\infty(t) + [\epsilon(t) - \epsilon_\infty(t)] \int_0^\infty \exp(-i\omega t') \left[\frac{-\partial \phi(t')}{\partial t'} \right] dt' \quad (14)$$

$$\epsilon^*(t) = \epsilon_\infty(t) + [\epsilon(t) - \epsilon_\infty(t)] N^*(i\omega t) \quad (14a)$$

$$N^*(i\omega t) = N'(\omega t) - iN''(\omega t) = \mathcal{L} \left(-\frac{\partial \phi}{\partial t'} \right) \quad (14b)$$

where $\epsilon_0(t)$ and $\epsilon_\infty(t)$ are the limiting low- and high-frequency values of permittivity, $\phi(t')$ is the dielectric relaxation function at any instant of cure, t' is the time for the observation of the decay of the response to an electric field, and \mathcal{L} represents a one-sided Laplace transform. For a measurement frequency of 1 kHz, the response time, t' , is on the order of 1 ms, during which time the physical changes in the state of the thermoset are justifiably assumed to be negligible.

Further derivations from eq 14, which are given in detail in the succeeding paper, show that the response of the complex dielectric permittivity, ϵ^* , is the same whether the variable of one's choice is frequency, ω , or the relaxation time, τ . That is, the shapes of the complex plane plots of ϵ'' against ϵ' are the same whether measurements are made with time during a continuous chemical change, which increases τ , or are made with increasing frequency of a chemically stable substance. In our studies of the dielectric properties of thermosets measured for a fixed frequency during their isothermal curing, τ becomes an independent variable, which changes as the physical state of the thermoset changes. Furthermore, $\phi(t)$ is represented as a stretched exponential decay by³

$$\phi(t) = \exp[-t/\tau(t)]^\gamma \quad (15)$$

where γ is the new parameter applicable for the behavior of a thermoset during its curing. The new parameter was introduced to distinguish it from the Kohlrausch-Williams-Watts parameter, β , used in the characterization of the relaxation process in chemically and physically stable materials.

With our ϵ' and ϵ'' data at 1-kHz measuring frequency, obtained for the two thermosets during their curing, we now examine the validity of the relaxation function, or eq 15. In order to do so, it is necessary to know both $\epsilon'(t \rightarrow 0)$ and $\epsilon'(t \rightarrow \infty)$. These quantities are the short- and long-time intercepts of the complex plane plot of the experimental ϵ'' against ϵ' . The curing parameter, γ , was then evaluated from the values of N'_m and N''_m , which represent the real and imaginary components of the normalized

Table II
Various Parameters Used for Calculating the Dielectric Properties of DGEBA-Based Thermosets Measured during Their Isothermal Curing at Different Temperatures

T/K	t_{gel}/ks	x	$\sigma_0(t \rightarrow 0)/(\mu S/cm)$	t_0/ks	$A/(S/cm)$	B/ks	$\epsilon'(t \rightarrow \infty)$	$\epsilon'(t \rightarrow 0) - \epsilon'(t \rightarrow \infty)$	γ
DGEBA-PDA									
294.9	12.2	3.35	67.20	20.4	0.015	110.9	4.5	5.15	0.31
303.8	6.20	2.63	140.0	9.10	0.004	31.5	4.6	4.5	0.29
315.5	3.40	3.84	242.0	5.30	0.067	29.6	4.5	3.95	0.28
323.7	2.01	3.98	538.0	3.05	0.128	16.8	4.6	3.5	0.28
335.0	1.10	4.17	1064	1.58	0.172	8.20	4.7	3.05	0.27
346.0	0.63	4.38	2212	0.84	0.157	3.81	4.6	2.6	0.27
DGEBA-HMDA									
284.3							4.5	4.85	0.32
296.5	12.2	3.22	35.30	18.6	0.003	85.43	4.5	4.35	0.32
304.2	7.45	3.2	54.70	11.5	0.005	52.81	4.5	3.90	0.32
312.3	4.30	3.27	88.20	7.40	0.023	41.24	4.45	3.48	0.31
324.2	2.16	3.61	162.5	3.20	0.028	15.34	4.6	3.0	0.30
336.5	1.26	3.92	435.0	1.75	0.036	7.95	4.65	2.45	0.30

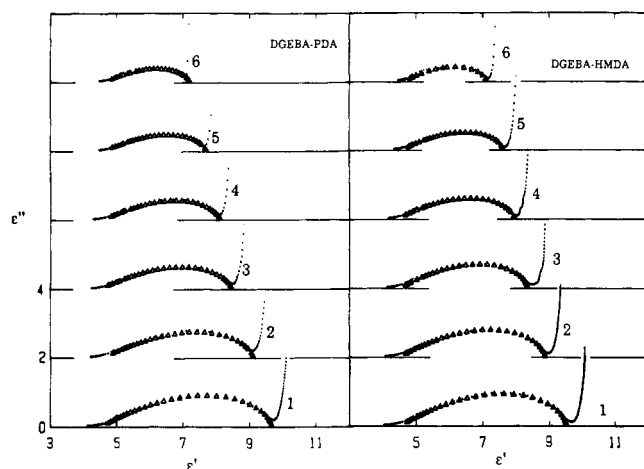


Figure 5. Complex plane plots of ϵ'' against ϵ' for the DGEBA-PDA and DGEBA-HMDA thermosets, measured at a frequency of 1 kHz, during their isothermal curing. The numbers next to the curves correspond to the curing temperatures as listed in Table I. The triangles were calculated using eq 15 and the parameters listed in Table II.

permittivity at the maximum value of N''_m , according to the equations

$$N'(\omega\tau(t)) = \frac{\epsilon'(\omega\tau(t)) - \epsilon'(t \rightarrow \infty)}{\epsilon'(t \rightarrow 0) - \epsilon'(t \rightarrow \infty)}; \quad N'_m = \frac{\epsilon'_m - \epsilon_\infty}{\Delta\epsilon} \quad (16)$$

$$N''(\omega\tau(t)) = \frac{\epsilon''(\omega\tau(t))}{\epsilon'(t \rightarrow 0) - \epsilon'(t \rightarrow \infty)}; \quad N''_m = \frac{\epsilon''_m}{\Delta\epsilon} \quad (17)$$

where ϵ'_m is the value of ϵ'_{peak} given in Table I for the respective thermosets, $\Delta\epsilon = (\epsilon'(t \rightarrow 0) - \epsilon'(t \rightarrow \infty))$ and ϵ'_m is the permittivity, at the time when ϵ'_{peak} appears.

The evaluation of the integral form of $N''(\omega\tau)$ is necessary for discussing the permittivity data. Moynihan et al.⁹ have calculated N'' for various values of γ (they have given tables listing both N' and N'' as functions of ω and τ , for the product, $z = \omega\tau$, ranging in values from 10^{-3} to 10^6 , as a function of the parameter γ or β , from 0.3 to 1.0. For values of β or $\gamma < 0.3$, similarly extended tables have been provided by Dishon et al.¹³ listing N' and N'' for values of the product $z = \omega\tau$ from 10^{-3} to 10^8 . These tabulated values were used to calculate from eqs 16 and 17 ϵ' and ϵ'' for DGEBA-PDA and DGEBA-HMDA thermosets during their curing. The calculated values are shown as triangles along with the experimental values measured for 1 kHz in the complex plane plots of ϵ'' against ϵ' in Figure 5. The agreement between the calculated and measured values is excellent for both thermosets during

their curing at different temperatures with systematic deviations occurring only at long curing times, when the dielectric loss, $\epsilon''(t \rightarrow \infty)$, instead of approaching zero, remains finite. The values of the parameters used for the calculations, namely, $\epsilon'(t \rightarrow 0)$, $\epsilon'(t \rightarrow \infty)$, and γ , are listed in Table II for each isothermal curing temperature for the two thermosets.

(d) Time Dependence of the Dielectric Relaxation Process. As the molecular structure of a thermosetting polymer irreversibly changes during its cure as a result of a negative feedback between the chemical reaction and molecular diffusion, its relaxation time increases. A method for obtaining its value at any instant of isothermal cure, in the postgel region, has been outlined by Johari and Mangion.³ Since the complex plane plots of the complex dielectric permittivity, ϵ^* , have been shown in Figure 5 to be well-described by a stretched exponential function with a characteristic distribution parameter, γ , each calculated data point, denoted by triangles in Figure 5, corresponds to a unique value of the normalized complex permittivity, N^* , which in turn corresponds to a unique value of ϵ' and ϵ'' according to eqs 16 and 17. Since the frequency of measurement is fixed, N^* becomes a unique function of the relaxation time, τ . Thus each calculated value of ϵ' and ϵ'' corresponds to a characteristic relaxation time, τ . The relaxation time is now evaluated by matching the values of ϵ' and ϵ'' from eqs 16 and 17 with the experimental ϵ' and ϵ'' at a given instant of curing. When the calculated values of ϵ' and ϵ'' did not correspond to the time at which ϵ' and ϵ'' were measured, values were linearly interpolated from the closest measured values. The relaxation time for each instant of cure was then calculated from the $(\omega\tau)$ values given for a set $N'(\omega\tau)$ and $N''(\omega\tau)$ in the tables by Moynihan et al.⁹ Since Moynihan et al. calculated the values for $\omega\tau$ in the range 10^{-3} to 10^6 , the relaxation time values were limited to 10^{-2} to 10^7 s. These values for τ are plotted against the curing time in Figure 6 for the DGEBA-PDA and DGEBA-HMDA thermosets.

The correctness of this method may be examined by evaluating the values of ϵ' and ϵ'' using the calculated relaxation time data and eqs 16 and 17. This was done, and the fit to the data is shown as plots of ϵ' and ϵ'' against the curing time in Figure 6 for the two thermosets. The agreement between the calculated and experimental values for all curves suggests that the method for determining relaxation time is satisfactory.

In Figure 6, the plots of relaxation time against log (curing time) have qualitatively similar shapes for all of the temperatures of cure for each thermoset, with the shape being sigmoidal with an expected approach toward a plateau at long times as the thermoset becomes a vitreous

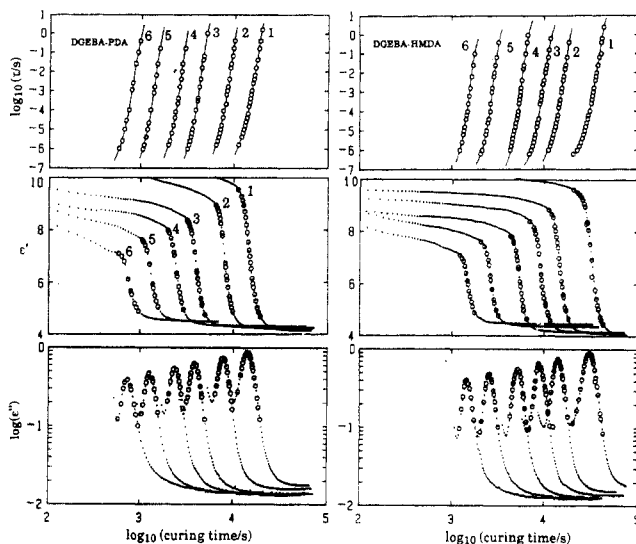


Figure 6. Relaxation times of the DGEBA-PDA and DGEBA-HMDA thermosets, as calculated from the permittivity data measured at a frequency of 1 kHz, plotted against time for their isothermal curing. The numbers next to the curves correspond to the curing temperatures as listed in Table I. The permittivity and loss are also plotted against time. The circles are the data calculated from the formalism.

solid. As the temperature of the cure is raised, the curves are broadened, such that the slope $(\partial \log \tau / \partial \log t)_T$ at the inflection point of the curve decreases. The shape of the plots of $\log(\tau)$ against $\log(\text{curing time})$ is also remarkably similar for both thermosets, suggesting that the structural changes that occur during the isothermal curing of thermosets are similar for each system and thus are independent of the molecular length and nature of the curing agent used. Theoretical implications of these results will be discussed in more detail in the discussion later here.

The gelation time t_{gel} was calculated for each temperature of isothermal curing of the two thermosets. For each system, the relaxation time at gelation is seen to increase as the temperature of the isothermal cure is raised. This implies that, as the temperature of isothermal cure is increased, the structure of the thermoset at the gelation point becomes more densely cross-linked and subsequently has a longer relaxation time. These observations will be further discussed in terms of the mechanisms of reaction in section IV(iv).

(ii) Isothermal Curing Kinetics Measured at Different Frequencies. In the discussion of the isothermal curing of DGEBA in section IV(i), with molecularly linear diamine curing agents, the dielectric properties were analyzed in terms of contributions from both ionic conductivity and dipolar reorientation. The analysis showed that their ionic conductivity is equally well described by either a power law (eq 12) or a singularity equation (eq 13), both of which can account for the approach of the conductivity toward a singularity, but at different times t_{gel} and t_0 , respectively. In order to resolve whether the time for gelation deduced from the analysis of ionic conductivity is a material property or an artifact of the measurement, it is necessary to examine the effect of the frequency of measurement on the values of t_{gel} and t_0 , because, for a material property, the values of t_{gel} and t_0 would be independent of the frequency of measurement. Furthermore, it would help resolve the extent to which the contribution of the dipolar relaxation to the conductivity remains significant for different frequencies. Therefore, the dielectric properties were measured at three

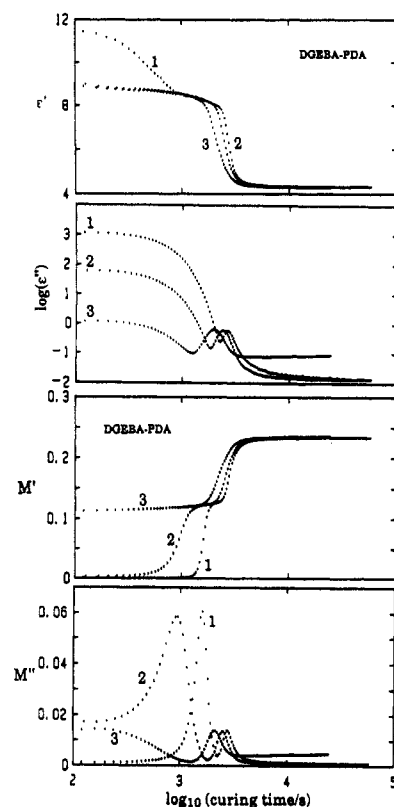


Figure 7. Dielectric permittivity and loss, and the real and imaginary components of the complex electrical modulus M' and M'' , of the DGEBA-PDA thermoset measured during its isothermal curing at 324 K, plotted against time for measurements made at the following frequencies: (1) 50 Hz, (2) 1 kHz, (3) 50 kHz.

different frequencies for both thermosets during their isothermal cure. The dielectric properties of the DGEBA-PDA and DGEBA-HMDA thermosets measured at 50 Hz, 1 kHz, and 50 kHz during their isothermal curing at 313.5 and 305.2 K respectively are plotted against $\log(\text{curing time})$ in Figures 7 and 8. Evidently, the changes in ϵ' , ϵ'' , M' , and M'' in the plots for the two thermosets are remarkably similar. For both thermosets at short times of their cure, ϵ' slightly decreases, approaching a plateau value as the curing time increases. The initial decrease is more pronounced for measurements at 50-Hz frequency. As seen in Figures 7 and 8, the plateau is interrupted by a step decrease, following which there is an approach to a limiting value, $\epsilon'(t \rightarrow \infty)$, at long times. As the frequency of measurement is increased, the step appears at shorter times, while its magnitude remains relatively constant. ϵ'' begins at a near plateau value during the initial stages of cure, with the plateau decreasing to a minimum as the time of cure increases. Following the minimum, ϵ'' increases, reaches a peak value, and subsequently decreases toward a limiting value at long time, denoted as $\epsilon''(t \rightarrow \infty)$. As the frequency of measurement is increased, the heights of the initial plateau and local minimum decrease, while the corresponding heights of the peak and the long-time limiting value, $\epsilon''(t \rightarrow \infty)$, increase, and the corresponding minimum and peak positions are shifted to shorter times.

The plot of M' against $\log(\text{curing time})$, shown in Figures 7 and 8, is seen to increase in two steps toward a limiting value for the 50-Hz frequency measurements and in one step for 1- and 50-kHz measurements. The position of the step toward the limiting long-time value, M_∞ , shifts toward shorter times as the frequency of measurement increases, while its corresponding magnitude remains constant.

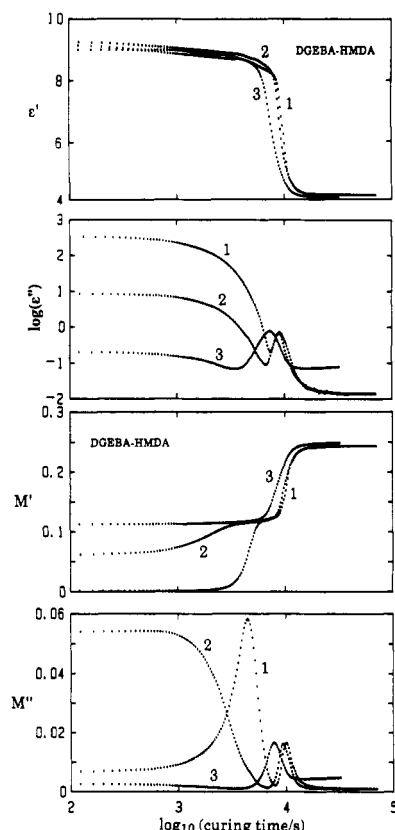


Figure 8. Dielectric permittivity and loss, and the real and imaginary components of the complex electrical modulus M' and M'' , of the DGEBA-HMDA thermoset measured during its isothermal curing at 324 K, plotted against time for measurements made at the following frequencies: (1) 50 Hz, (2) 1 kHz, (3) 50 kHz.

The plot of M'' against \log (curing time) shows two peaks for the 50-kHz frequency measurement. The height of the first peak decreases for the 1-kHz measurement, and the peak vanishes for the 50-kHz measurement. The position of the second peak shifts to shorter times, and its magnitude increases as the frequency is increased. The value of M'' at long times, $M''(t \rightarrow \infty)$, increases as the frequency of measurement is increased.

The positions of the minimum and the peak in the plots of ϵ'' shift to shorter times as the frequency is increased, and the corresponding magnitudes of the minimum, the peak, and the limiting long-time value increase. The values of $t_{\text{peak}}(\epsilon'')$, $\epsilon''(t \rightarrow \infty)$, $\epsilon'(t \rightarrow \infty)$, and $\epsilon'(t \rightarrow 0)$ for different frequencies of measurement for the isothermal curing of the two thermosets are given in Table III.

(iii) Conductivity and Dipolar Relaxations. The results obtained for the different frequencies during the isothermal curing of thermosets are analyzed similarly to those for the 1-kHz frequency, already described here, and the complex plane plots of M' and M'' are shown in Figures 9 and 10. The parameters x , t_{gel} , and $\sigma_0(t \rightarrow \infty)$ used for the power law and A , B , and t_0 used in the singularity equation were calculated from eqs 12 and 13 and are compared against the experimental data in the plots of $\log \sigma$ against \log (time) in Figures 11 and 12 for the DGEBA-PDA and DGEBA-HMDA thermosets, respectively. Evidently, σ_0 calculated from both equations agrees with the measured σ_0 , with deviations occurring at times close to the time when σ reaches a minimum value and when the dipolar affects contribute significantly. The values of t_{gel} during the isothermal curing of the DGEBA-PDA thermoset at 323 K are 2.3, 2.01, and 1.9 ks from measurements made at frequencies of 50 Hz, 1 kHz, and 50 kHz, respectively. For the isothermal curing of the

DGEBA-HMDA thermoset at 305 K, the values of t_{gel} are 7.55, 7.45, and 7.20 ks. Evidently the values of t_{gel} are constant to within 5% over a frequency range of 2–3 decades. This confirms our expectation that the singularity point or t_{gel} is independent of the frequency used for the measurement. Furthermore, the values of $\sigma_0(t \rightarrow 0)$ and t_0 are constant to within 7% with changing frequency. The parameters x , t_{gel} , $\sigma_0(t \rightarrow 0)$, A , B , and t_0 for the different thermosets for the different frequencies of measurements are summarized in Table III.

The ϵ' and ϵ'' due to the dipolar relaxation process are fitted to a stretched exponential function of eq 15, according to the method already described here. The calculated values are shown in the plots of ϵ'' against ϵ' in Figures 9 and 10 for the DGEBA-PDA and DGEBA-HMDA thermosets, respectively. For the DGEBA-PDA thermoset, the values of $\Delta\epsilon$ are 3.5, 3.5, and 3.75 for the measurements made at 50 Hz, 1 kHz, and 50 kHz, respectively. For the DGEBA-HMDA thermoset, the values of $\Delta\epsilon$ are 3.65, 3.8, and 4.0 for measurements made at the corresponding frequencies. The values of $\epsilon'(t \rightarrow 0)$ and $\epsilon'(t \rightarrow \infty)$ are also listed in Table III. They show that the change in ϵ' during a thermoset's curing remains constant irrespective of the frequency used for the measurement and thus confirm the correctness of the procedure and the formalism used here.

Frequency Dependence of the Relaxation Time. The relaxation time of the thermoset was determined by using the stretched exponential function or eq 15. The method is already described here. The results are shown as plots of $\log \tau$ against \log (curing time) in Figure 13 for the DGEBA-PDA and DGEBA-HMDA thermosets. For each thermoset, calculated relaxation times from measurements at the three frequencies lie on the same curve whose range in τ is now extended to cover from 10^{-9} to 10^2 s. This extension has been possible from the extended range of frequencies used in these measurements.

The results from the study of the frequency dependence of dielectric behavior of thermosets during their curing are summarized as follows: (i) the time t_{gel} and $\sigma_0(t \rightarrow 0)$ are independent of the frequency of measurement, which shows that the assumption that dc conductivity is the dominant dielectric effect during the early stage of isothermal curing is correct; (ii) the times at which the peaks in ϵ'' and M''_{dip} appear increase on a decrease in the frequency of measurement and a decrease in ϵ' on curing and the curing parameter remains constant, which show that the parameters $\Delta\epsilon$ and γ are temperature-dependent only and remain unchanged during the isothermal curing; (iii) the single plot of relaxation time against \log (curing time) shows that it is the changes in the relaxation time which determine the dielectric properties of a thermoset during its isothermal cure. Other effects are relatively insignificant.

The parameters t_{gel} and t_0 are the times for σ_0 to reach a formal but unattainable zero value in the power law and singularity equations. In section VI.(1)(b), we have shown that t_{gel} is less than $t_{\text{peak}}(\epsilon'')$ while t_0 is greater than $t_{\text{peak}}(\epsilon'')$ for the 1-kHz frequency measurements. When different frequencies are used, the values of t_{gel} and t_0 listed in Table III show the same pattern, namely, $t_{\text{gel}} < t_{\text{peak}}(\epsilon'') < t_0$, and t_0 represents a singularity point which occurs at long times of cure. However, the dielectric loss, ϵ'' , at the corresponding times t_0 is relatively high as noted in Table III. Since the dielectric properties in the vitreous state are seen to remain constant with time, for isothermal measurements, the time t_0 cannot be the vitrification time of the thermoset. Similarly, since t_0 is greater than $t_{\text{peak}}(\epsilon'')$, it corresponds

Table III
Features of the Dielectric Behavior of DGEBA-Based Thermosets and the Parameters Used for Calculating Their Dielectric Properties at Several Frequencies during Their Isothermal Curing at the Temperature Indicated

freq/kHz	$\epsilon'(t \rightarrow 0)$	$\epsilon'(t \rightarrow \infty)$	$t_{\text{peak}}(\epsilon'')$	$\epsilon''(t \rightarrow \infty)$	$\sigma(t \rightarrow 0)/(\mu\text{S/cm})$	x	t_{gel}/ks	$A/(\text{S/cm})$	B/ks	t_0/ks
DGEBA-PDA (Curing at 323.7 K)										
0.05	8.0	4.5	2.65	0.0133	507.0	4.55	2.30	0.198	20.5	3.40
1.0	8.1	4.6	2.4	0.0133	538.0	3.98	2.01	0.128	16.8	3.05
50.0	8.3	4.55	1.95	0.0833	465.0	3.12	1.85	0.044	13.2	2.90
DGEBA-HMDA (Curing at 304.2 K)										
0.05	8.1	4.45	9.45	0.0155	48.0	3.40	7.55	0.007	57.61	11.7
1.0	8.35	4.5	9.05	0.0151	54.7	3.20	7.45	0.005	52.81	11.5
50.0	8.55	4.55	7.20	0.075	57.0	2.11	7.10	0.001	36.13	11.3

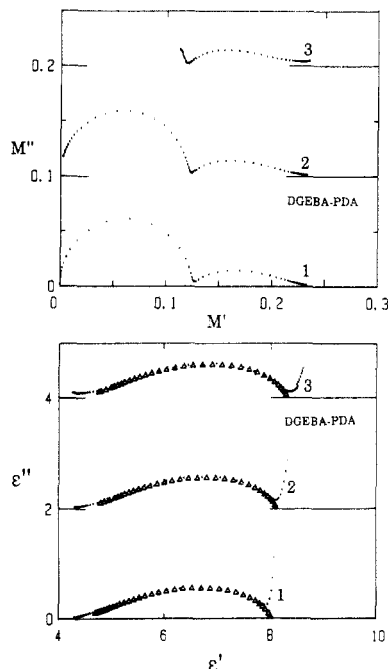


Figure 9. Complex plane plots of M'' and M' and ϵ'' and ϵ' for the DGEBA-PDA thermoset measured during its isothermal curing at 324 K, for measurements made at the following frequencies: (1) 50 Hz, (2) 1 kHz, and (3) 50 kHz. The triangles were calculated using eq 15, and the parameters are listed in Table III.

to far longer times than the time for the singularity at gelation. For these reasons, we prefer the power law equation which implies a singularity at, t_{gel} , the gelation time. The fit of the data to both equations suggests that the two equations are indistinguishable over a certain small range of time for measurement. A critical evaluation of these conditions with relevance to temperature dependence has been given by Pathmanathan and Johari.¹⁴

(iv) Curing Kinetics and the Chain Length of the Curing Agent. During the curing of a thermoset, the rate of chemical reaction depends on the rate of the rotational-translational diffusion of the reacting species, i.e., the epoxide and amine groups. For a thermoset cured with a linear diamine as a curing agent, this diffusion is of two types, namely, (a) the diffusion of the free diamine molecule and of the partly reacted diamine-DGEBA oligomer and (b) the diffusion of the end groups of the diamine-DGEBA oligomer or the diamine with one of its ends fixed to the network or chain. To investigate the differences in these diffusion processes for curing agents of different molecular size, we now compare the results for the different diamine cured thermosets. The parameters $\sigma(t \rightarrow 0)$, t_{gel} , x , and γ listed in Tables II and III, which were used to describe the data according to eqs 14 and 15 and the measured values of $\Delta\epsilon$ and $t_{\text{peak}}(\epsilon'')$, are plotted against the reciprocal of curing temperature in Figure 14 for the DGEBA-PDA and DGEBA-HMDA thermosets.

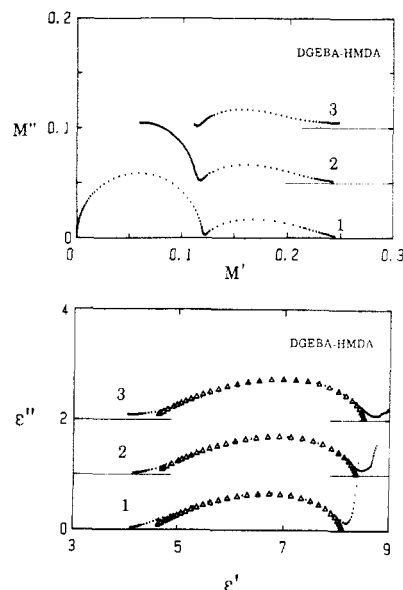


Figure 10. Complex plane plots of M'' and M' and ϵ'' and ϵ' for the DGEBA-HMDA thermoset measured during its isothermal curing at 350 K, at the following frequencies: (1) 50 Hz, (2) 1 kHz, (3) 50 kHz. The triangles were calculated using eq 15, and the parameters are listed in Table III.

The plots of t_{gel} against the reciprocal of temperature appear to show an exponential increase with temperature. These data were therefore fitted to an equation of the form

$$t_{\text{gel}} = A \exp(B/T) \quad (18)$$

where A and B are empirical parameters. The plots t_{gel} against $1/T$ are shown in Figure 15, where for each thermoset the curves are seen to have qualitatively similar shapes. The values of parameter A are 2.84×10^{-5} and 4.8×10^{-5} s for the DGEBA-PDA and DGEBA-HMDA thermosets, respectively, and the corresponding values of B are 5854 and 5730 K⁻¹. The dielectric data for the isothermal curing of the DGEBA-DDM and DGEBA-DDS thermosets obtained by Mangion¹⁵ have also been analyzed according to eq 18, and the plots of their t_{gel} against $1/T$ are also shown in Figure 15. In the time-temperature-transformation (TTT) diagram suggested by Enns and Gillham¹⁶ where the curing behavior of a model thermoset is qualitatively shown as a function of the curing temperature, the gelation curve, representing the time to reach gelation at different curing temperatures, seems to follow an exponential relation similar to that given by eq 18. Evidently, the temperature dependence of the gelation time obtained from the analysis of dielectric data qualitatively agrees with that of previous studies by Enns and Gillham¹⁶ using torsional braid analysis.

However, there are exceptions to this qualitative shape for the gelation-time temperature curves, as an analysis of the dielectric data for the curing kinetics of DGEBA

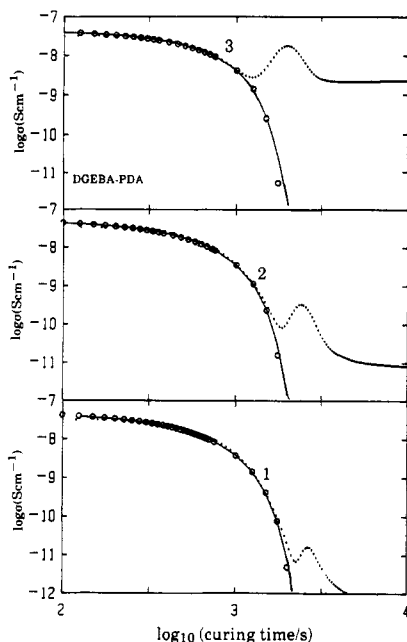


Figure 11. Conductivity of the DGEBA-PDA thermoset measured during its isothermal curing at 324 K plotted against time for measurements made at the following frequencies: (1) 50 Hz, (2) 1 kHz, (3) 50 kHz. The circles are the data calculated from the power law, and the full lines are those calculated from the singularity equation, using the parameters listed in Table III.

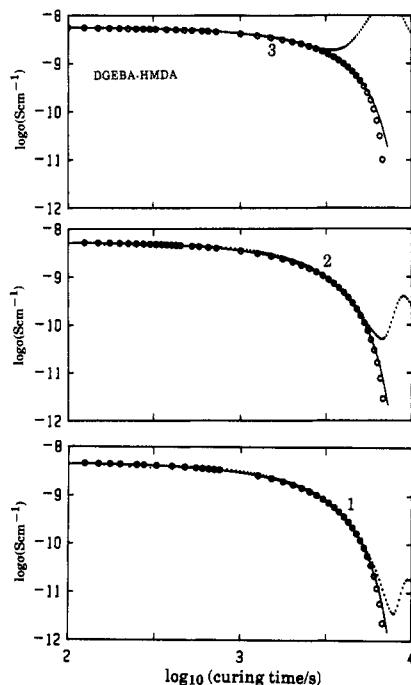


Figure 12. Conductivity of the DGEBA-HMDA thermoset measured during its isothermal curing at 305 K plotted against time for measurements made at the following frequencies: (1) 50 Hz, (2) 1 kHz, and (3) 50 kHz. The circles are the data calculated from the power law, and the full lines are those calculated from the singularity equation, using the parameters listed in Table III.

with dimethylbutylamine used as a catalyst by Alig and Johari¹⁷ shows. The plot of t_{gel} against the reciprocal of the curing temperature in Figure 15 shows that for lower temperatures of curing the plot is linear but for higher temperatures the plot curves inward such that t_{gel} now increases as the curing temperature is increased. In Enns and Gillham's TTT diagrams,¹⁸ this type of behavior occurs only in the curves of vitrification time; i.e., as T_{cure} approaches the ultimate glass transition temperature, $T_{\text{g}\infty}$, the curve's shape changes, with the time for vitrification

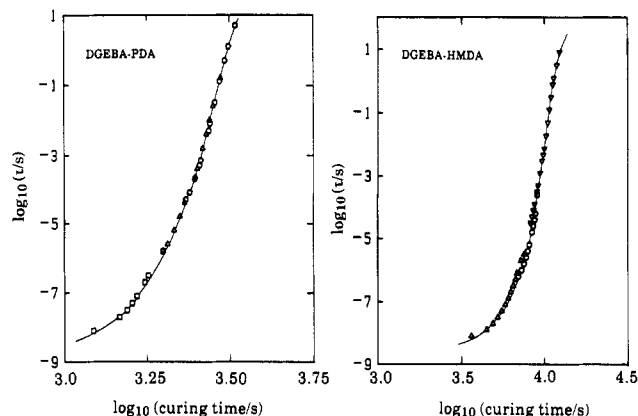


Figure 13. Relaxation times of the DGEBA-PDA and DGEBA-HMDA thermosets during their curing at 324 and 305 K, respectively, plotted against time. The data correspond to measurements made at (□) 50 Hz, (Δ) 1 kHz, and (○) 50 kHz.

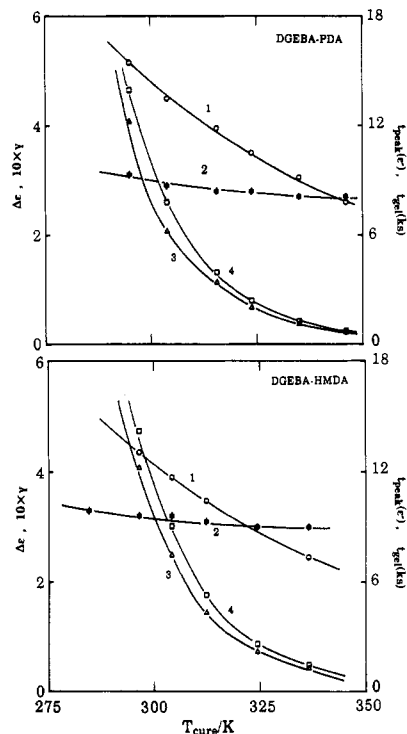


Figure 14. Temperature dependence of the dielectric parameters obtained from the isothermal curing of the DGEBA-PDA and DGEBA-HMDA thermosets. The notation is as follows: (1) $\Delta\epsilon$, (2) γ , (3) t_{gel} , (4) $t_{\text{peak}}(\epsilon'')$.

increasing as the curing temperature is increased. We propose that the curve for gelation follows a similar behavior, so that at low curing temperatures the data are described by eq 18, but at high curing temperatures the curve bends much like the vitrification curve. Additional studies over a wide range of curing temperatures are required to test this prediction.

The dc conductivity of the unreacted thermoset liquid, or $\sigma(t \rightarrow 0)$, listed in Table II decreases with an increase in the chain length of the curing agent at the same temperature. This decrease seems consistent with the suggestion that dc conductivity results from the diffusion of free impurity ions in the liquid, and, as the molecular length of the curing agent is increased, both its melting point and viscosity increase, the increase in the latter reducing the ionic mobility according to the Stokes-Einstein equation.

We now discuss the dependence of γ on the curing temperature and the chain length of the curing agent. Figure 15 shows that its value decreases toward a limiting value

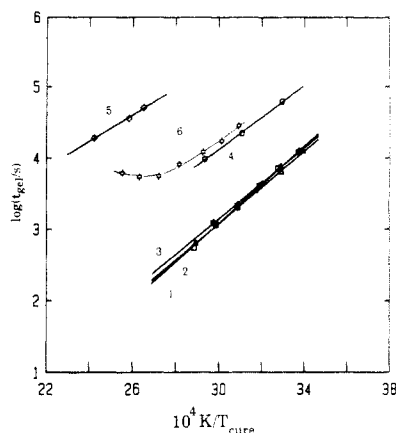


Figure 15. Time for gelation plotted against the reciprocal of temperature for the isothermal curing of thermosets. Full lines were calculated from eq 18 using the parameters listed in Table II and are drawn for (1) the DGEBA-EDA thermoset,⁵ (2) the DGEBA-PDA thermoset, (3) the DGEBA-HMDA thermoset, (4) the DGEBA-DDM thermoset,¹⁻⁴ (5) the DGEBA with dimethylbutylamine,¹⁷ and (6) the DGEBA-DDS thermoset.¹⁻⁴

as the temperature of cure is increased. Similar behavior has been reported for DGEBA-DDM thermosets by Mangion and Johari.¹⁻⁴ For a given thermoset, a decrease in γ with an increase in the curing temperature implies that, for thermosets cured at different temperatures, the extent of reaction for a given curing temperature is higher at higher temperatures and the thermoset formed has a higher cross-link density and lower γ . Recent studies using mechanical relaxation and calorimetry by Mikolajczak et al.¹⁸ and Hofer and Johari¹⁹ also show that the number of cross-links formed increases with the temperature of cure.

A comparison of γ at a fixed temperature of cure for the three curing agents, EDA,⁵ PDA, and HMDA, shows that γ increases with the molecular length of the curing agent. With curing agents of long molecular length, one intuitively expects that the molecular network formed would be more loosely packed, since the inter-cross-link distance would be greater than in that formed with small size curing agents. For such cases, γ becomes an indicator of the packing density of the thermoset. These studies predict that, for higher packing density, i.e., for increased cross-linked density of the ultimately formed thermoset, γ , during its curing, would be found to be low, an observation also deduced from the dependence of γ on the curing temperature.

(v) Thermoset's Cure and Frequency-Dependent Properties. The relaxation times during the isothermal curing of thermosets, obtained from measurements made at several different frequencies, lie on a single plot of $\log \tau$ against \log (curing time). Thus the dielectric properties of a thermoset at any instant of its curing correspond to the relaxation time of the thermoset's structure at that instant and are independent of the frequency used in the measurement. Studies of the dielectric properties of materials with a fixed structure by Johari and Goldstein²⁰ and Johari²¹ have shown that molecular relaxation in an amorphous material occurs with at least a bimodal distribution of relaxation times which corresponds to the α and β relaxations. When the measurement temperature T is near or below T_g , both relaxation processes are observed within the frequency range generally available, but when $T < T_g$, only one relaxation, namely, the β process, is observed. As curing of a thermoset progresses, its physical structure changes from that of a liquid when $T_{\text{cure}} > T_g$ to that of a vitreous solid when $T_{\text{cure}} < T_g$.

For measurements made at a fixed frequency during the curing process, one would observe a continuous change

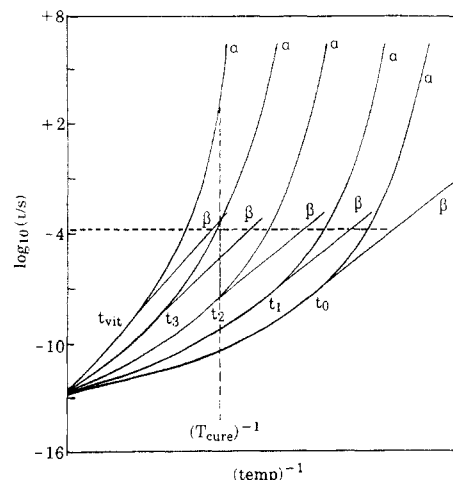


Figure 16. Illustration of the change in the relaxation times for the α - and β -relaxation processes of the network structure at a given instant of cure t_{cure} . For simplicity, the plots are drawn to have the same slope and to merge at a frequency of 10^7 Hz. The preexponential factor for all plots is the same.

in the properties as the structural state of a thermoset continuously evolves and traverses with time from the one with a relaxation time of a fluid, say, 10^{-9} s, to one with a very long relaxation time, say, 10^4 s, of its vitreous state. This is illustrated in Figure 16 where the anticipated increase in the relaxation time for the α - and β -relaxation processes with decreasing temperature is illustrated for measurements made at different instants $t_0, t_1, t_2 - t_{\text{vit}}$, etc. For clarity, the plots of the β -relaxation process are drawn to have the same slopes and to merge, as has been found earlier, at a frequency of measurement of 10^7 Hz. The preexponential factor of 10^{12} Hz is necessarily kept the same for all plots as it corresponds to the vibrational frequency of atoms. In Figure 16 the measured ϵ' and ϵ'' at 1-kHz frequency would initially correspond to a structure and a relaxation rate at a point T_{cure}^{-1} on curve t_0 . As time increases, the thermoset properties change which corresponds to the structure and relaxation times for points along a vertical line at T_{cure}^{-1} on curves t_1, t_2, t_3, \dots , etc., and ultimately on the curve t_{vit} , the vitrification time. As t_{vit} is reached, all contributions from the α -relaxation process may not yet have reached their minimum value if the frequency of measurement corresponds to the β -relaxation rate of the network structure. Previous studies by Mangion and Johari²² and Sidebottom and Johari²³ have shown that the strength of the β relaxation initially increases with time during the post-curing. Simultaneously, the α -relaxation process shifts to lower frequencies and thus its contribution to ϵ'' decreases. In measurements made at a fixed instant after t_{vit} where postcure occurs sufficiently slowly to allow the measurement of the frequency spectrum, one would find, as shown by Mangion and Johari,²² a peak in the frequency spectrum of ϵ'' and a shift of the position of the β -relaxation peak toward high frequencies with an increase in the temperature. Alternatively, for isothermal curing done at a fixed temperature and different frequencies used for measurement of the thermoset dielectric properties, the measured ϵ'' is frequency-dependent, showing a peak whose position shifts to a higher frequency with an increase in the temperature of the isothermal cure. That this does occur is shown in Figure 17, where ϵ' and ϵ'' of a typical thermoset, DGEBA-ethylenediamine, especially measured for obtaining the dielectric properties at a fixed time, are plotted against the time for five measurement frequencies.

The dielectric behavior during the isothermal curing of the DGEBA-PDA and DGEBA-HMDA thermosets an-

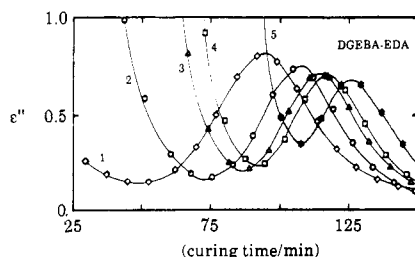


Figure 17. Dielectric loss for the DGEBA-EDA thermoset measured during its isothermal curing at 305 K plotted against time for the following frequencies of measurement: (1) 0.05, (2) 0.5, (3) 1, (4) 5, (5) 50 kHz.

alyzed according to a stretched exponential relaxation function in terms of the complex plane plot of ϵ'' against ϵ' in Figures 9 and 10 shows that at long times $\epsilon''(t \rightarrow \infty)$ for a measurement frequency of 100 kHz does not reach zero and that this causes deviations in the fit of the experimental data to eq 15. We conclude that these deviations are caused by contribution from the β -relaxation process, which becomes significant as the thermoset's curing progresses.

$\epsilon''(t \rightarrow \infty)$ of the thermosets measured for the different fixed frequencies, but cured at the same temperature, is nearly 7 times higher for the high-frequency measurement than for the low-frequency measurement, as seen in Table III. This confirms our deduction that the increase in $\epsilon''(t \rightarrow \infty)$ with increasing frequency is due predominantly to the contributions from the β -relaxation process for which ϵ' has not reached its limiting high-frequency value and that $\epsilon''(t \rightarrow \infty)$ increases when a high frequency is used for the measurements, for the contribution to ϵ'' from the β -relaxation process for that frequency and temperature increases in the vitrified thermoset. Any further change in ϵ'' with time would be a reflection of the effects of further chemical reactions, known as postcure, on the strength of the β -relaxation process, as has been discussed in earlier papers.^{22,23}

V. Conclusions

A detailed dielectric study of the curing kinetics of DGEBA-based thermosets with propylenediamine and hexamethylenediamine during the sol \rightarrow gel to glass transformation shows time-dependent changes that can be understood in terms of dc conductivity, contribution to orientation polarization, and irreversible increase in the relaxation time. The decrease in dc conductivity, whose magnitude can be obtained from an analysis in terms of an electrical modulus, follows a power law used in the description of critical phenomena. Its exponent increases with an increase in the curing temperature, and the dc conductivity approaches a negligible value at the gelation time of the thermoset. Thus gelation can be characterized by dielectric measurements. An empirical equation based on an exponential decrease of the dc conductivity toward a singularity with curing time also fits the data, but the time for the singularity is closer to vitrification rather than the gelation time. The gelation time decreases as the inverse exponential of the temperature and with a decrease in the molecular size of the curing agent.

The evolution of the dielectric properties of thermosets during their curing is phenomenologically similar to the

evolution of the features of physically and chemically stable dipolar materials with increasing frequency of measurements at a constant temperature or with decreasing temperature at a constant frequency. The complex permittivity measured during the curing process can be fitted to a stretched exponential functional form, $\phi(t_{\text{cure}}) = \exp(-(t_{\text{cure}}/\tau)^\gamma)$, where γ , with values between 0.27 and 0.32, decreases with both an increase in the curing temperature and a decrease in the length of the curing agent. γ may be considered as a curing parameter for thermosets.

The relaxation time increases with the curing time, and the logarithmic plots show that its dependence is such that the plot is sigmoidal shape, with a point of inflection which shifts to shorter times with an increase in the curing temperature and a decrease in the chain length of the amine curing agent.

The dielectric properties measured for different fixed frequencies confirm the above-given observations.

Acknowledgment. This work constitutes part of the thesis for a McMaster of Science degree submitted by M.G.P. to the Graduate School in 1991. The work was supported by a grant from the Natural Sciences and Engineering Research Council of Canada.

References and Notes

- (1) Mangion, M. B. M.; Johari, G. P. *J. Polym. Sci., Part B: Polym. Phys.* **1990**, *28*, 1621.
- (2) Mangion, M. B. M.; Johari, G. P. *Macromolecules* **1990**, *23*, 3687.
- (3) Johari, G. P.; Mangion, M. B. M. *J. Non-Cryst. Solids* **1991**, *131*, 921.
- (4) Mangion, M. B. M.; Johari, G. P. *J. Polym. Sci., Part B: Polym. Phys.* **1991**, *29*, 1117, 1127.
- (5) Parthun, M. G.; Johari, G. P. *J. Polym. Sci., Part B: Polym. Phys.*, in press.
- (6) LeMay, J. D.; Swetlin, B. J.; Kelley, F. N. In *Characterization of Highly Crosslinked Polymers*; ACS Symposium Series 243; Labana, S. S., Dickie, R. S., Eds.; American Chemical Society: Washington, DC, 1984; p 65.
- (7) Choy, I. C.; Plazek, D. J. *J. Polym. Sci., Part B: Polym. Phys.* **1986**, *24*, 1303.
- (8) Macedo, P. B.; Moynihan, C. T.; Bose, R. *Phys. Chem. Glasses* **1972**, *13*, 171.
- (9) Moynihan, C. T.; Boesch, L. P.; Laberge, N. L. *Phys. Chem. Glasses* **1973**, *14*, 122.
- (10) Tombari, E.; Johari, G. P., submitted for publication in *J. Chem. Phys.*
- (11) Stauffer, D.; Coninglo, A.; Adam, M. *Adv. Polym. Sci.* **1982**, *44*, 105.
- (12) Djabourov, M. *Contemp. Phys.* **1988**, *29*, 273.
- (13) Dishon, M.; Weiss, G. H.; Bendler, J. T. *J. Res. Natl. Bur. Stand.* **1985**, *90*, 27.
- (14) Pathmanathan, K.; Johari, G. P. *Philos. Mag. B* **1990**, *62*, 225.
- (15) Mangion, M. B. M. Ph.D. Thesis, McMaster University, 1990.
- (16) Enns, J. B.; Gillham, J. K. *J. Appl. Polym. Sci.* **1983**, *28*, 2567.
- (17) Alig, I.; Johari, G. P. *J. Polym. Sci., Part B: Polym. Phys.*, in press.
- (18) Mikolajczak, G.; Cavaille, J.-Y.; Johari, G. P. *Polymer* **1987**, *28*, 2023.
- (19) Hofer, K.; Johari, G. P. *Macromolecules* **1991**, *24*, 4978.
- (20) Johari, G. P.; Goldstein, M. *J. Chem. Phys.* **1970**, *53*, 2372.
- (21) Johari, G. P. In *Molecular Dynamics and Relaxation Phenomena in Glasses*; Dorfmueller, Th., Williams, G., Eds.; Lecture Notes in Physics; Springer-Verlag: Heidelberg, Germany, 1987; p 90.
- (22) Mangion, M. B. M.; Johari, G. P. *J. Polym. Sci., Part B: Polym. Phys.* **1991**, *29*, 437.
- (23) Sidebottom, D. L.; Johari, G. P. *Chem. Phys.* **1990**, *147*, 205.